

# A COMBINED RADAR-RADIOMETER APPROACH TO ESTIMATE RAIN RATE PROFILE AND UNDERLYING SURFACE WIND SPEED OVER THE OCEAN

Shannon Brown and Christopher Ruf

University of Michigan  
2455 Hayward St. Ann Arbor, MI 48109, USA

## ABSTRACT

An algorithm is developed which combines the strengths of a 10.7 GHz microwave radiometer and a 13.4 and 35.6 GHz Doppler radar to retrieve the rain rate profile and the surface wind speed over the ocean. A dual-frequency radar algorithm is used to estimate two parameters of the gamma drop size distribution at each range gate. The precipitation extinction/absorption profile determined from the DSDs is used to remove the atmospheric contribution to the measured brightness temperatures in order to estimate the surface wind speed. Radiometric retrievals in light stratiform rain are driven by the absorption in the melting layer. Several melting layer models are compared by assessing how well they fit the radar measurements in the melting layer. A candidate model is chosen and its affect on the retrievals is analyzed.

## 1. INTRODUCTION

A retrieval algorithm has been developed which uses measurements of the backscattering coefficient from the PR-2 dual-frequency Doppler radar and horizontally polarized brightness temperature ( $T_B$ ) measurements from the LRR-X 10.7 GHz radiometer to simultaneously retrieve the vertical profile of precipitation and the near-surface wind speed. Results are presented from a field campaign in June of 2003 in which several DC-8 overflights were made in regions of stratiform and convective precipitation associated with a mid-latitude cyclone off the coast of Vancouver, British Columbia.

The retrieval algorithm uses the radar backscatter measurements at each frequency to iteratively solve for two parameters of the gamma drop size distribution (GDSD) at each radar range gate. In light rain, the measured backscatter is corrected for attenuation using a Hitschfeld-Bordan approach (Hitschfeld and Bordan 1954). In this way, the attenuation is corrected top-down, starting from the storm-top and progressing to the surface. The rain rate and liquid water content at each range gate are determined by integrating the parameterized GDSDs. The surface wind speed is determined from the 10.7 GHz  $T_B$ s by removing the atmospheric component and isolating the surface brightness, which monotonically increases with increasing surface wind speed. The atmospheric optical depth is determined by integrating the 10.7 GHz extinction coefficient determined at each range gate using Mie theory with the parameterized GDSDs. The surface emissivity is then found by inverting the radiative transfer equation and using the integrated optical

depth determined from the radar. A surface emissivity model is used to determine the near-surface wind speed.

In light stratiform rain, the melting layer, which is usually less than 600 m thick, can contribute up to 50 % of the atmospheric brightness, especially with low freezing levels. An example of this is shown in Figure 1 for 10.7 GHz. Therefore, the accuracy any microwave radiometer retrieval in stratiform rain is driven by the accuracy of the estimate of the absorption in the melting layer. Several melting layer models exist (Klassen 1988; Bauer et al. 1999; Bauer et al. 2000; Olson et al. 2001; Battaglia et al. 2003), and these are evaluated using the PR-2 and LRR data.

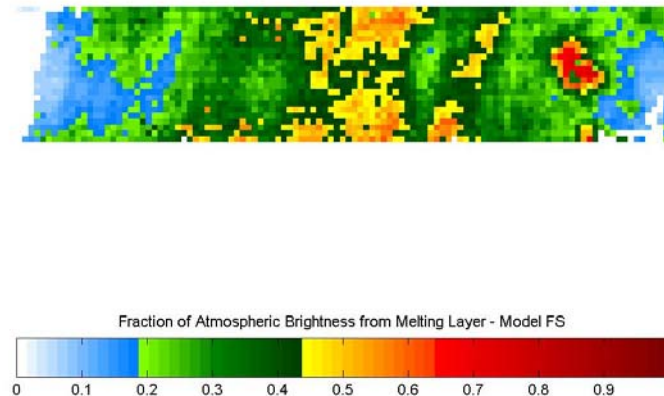


**Figure 1.** Fraction of the total atmospheric brightness from the melting layer at 10.7 GHz.

## 2. INSTRUMENT DESCRIPTION

The instruments used in this study are the JPL PR-2 Doppler radar, which operates at 13.4 and 35.6 GHz and the University of Michigan/GSFC LRR-X 10.7 GHz horizontally polarized radiometer. The PR-2 mechanically scans cross-track to  $\pm 25^\circ$  and LRR-X electronically images cross-track to  $\pm 45^\circ$ . The horizontal resolution of PR-2 is 800 m at the surface and LRR-X has a 500 m pixel resolution at the surface. The vertical resolution of PR-2 is 37 m. These instruments were integrated on a NASA DC-8 in June of 2003 at which time several overflights of precipitation were conducted.

## 3. MELTING LAYER MODELS

To determine the absorption and scattering in the melting layer one must use a thermodynamic model to determine the melted mass fraction as a function of height below the top of the layer and a dielectric mixing formula to determine the absorption and scattering coefficients for a given melting particle. The thermodynamic formula will drive the thickness of the melting layer and the choice of the dielectric model will determine the intensity of the absorption and scattering.

The melting rate of a snow particle that falls below the 273 K isotherm can be described in terms of a thermodynamic heating budget (Mitra et al. 1990). This provides the melted mass fraction at each height below the freezing level which is needed as input to a dielectric mixing formula. The melting rate for a particle is determined by the choice of the ventilation coefficient (Mitra et al. 1990, Szyrmer and Zawadzki 1999) and the initial snow density as well as the environmental

parameters, such as the temperature lapse rate and the relative humidity. A high lapse rate will cause the particle to melt faster. Contrary, if the relative humidity is low, the particle melting rate will slow due to the sensible heat being used to evaporate the melt water.

A commonly used formula to determine the dielectric of a mixture of air, ice and water is the Maxwell-Garnett (MG) mixing formula (Bohren and Battan 1982). The MG dielectric mixing formula is defined in terms of the dielectric constant of the two components, one being the matrix  $\epsilon_m$  and the other the inclusions  $\epsilon_i$ ,

$$\epsilon_{MG} = \frac{(1-f)\epsilon_m + f\beta\epsilon_i}{1-f + f\beta}, \quad (1)$$

where

$$\beta = \frac{2\epsilon_m}{\epsilon_i - \epsilon_m} \left[ \left( \frac{\epsilon_i}{\epsilon_i - \epsilon_m} \right) \text{Log} \left( \frac{\epsilon_i}{\epsilon_m} \right) - 1 \right],$$

Log() is the principal value of the complex argument and  $f$  is the volume fraction of the inclusions. For a three component mixture, such as a melting particle, the MG formula must be applied twice. The resulting dielectric will depend on the volume fraction of the three components and the order in which they are applied. The most often used forms are the  $MG_{wi}$  and the  $MG_{iw}$  (Bauer et al. 1999, Olson et al. 2001). The  $MG_{wi}$  is defined as a water matrix with inclusions of an ice matrix with air inclusions. The  $MG_{iw}$  is defined as inclusions of water in a matrix with a dielectric consisting of air inclusions in an ice matrix.. The following notation is defined to describe the different combinations used,

{matrix | inclusion}  $\rightarrow$  {matrix | {matrix | inclusion}}.

This gives  $MG_{wi} = \{\text{water} | \{\text{ice} | \text{air}\}\}$  and  $MG_{iw} = \{\{\text{ice} | \text{air}\} | \text{water}\}$ . The  $MG_{wi}$  is very similar to the dielectric of water and the  $MG_{iw}$  is more similar to that of snow. Recent comparisons with radar data have shown that the  $MG_{wi}$  consistently over estimates the peak of the bright band and the  $MG_{iw}$  consistently underestimates the peak of the bright band (Battaglia et al. 2003). Other models that have been used are { water | {air | ice}, { {water | ice} | air } (Klaassen 1988) and {air | {water | ice}} (Battaglia et al. 2003).

Another model which blends two MG mixing formulas is the Fabry and Szyrmer (1999) coated sphere model denoted FS. In this model, the melted particle is divided into a core and a shell that have different densities, but the same melted mass fraction. The dielectric of the shell is given by the MG formula {air | {water | ice}} and the dielectric of the core is given by { water | {air | ice}}. This produces a result that blends the strongly absorbing core with the weakly absorbing shell. The Fabry and Szyrmer model is a reasonable candidate, as it has compared favorably with radar profiler measurements in the melting layer (Battaglia et al. 2003).

#### 4. FITTING MELTING LAYER MODELS TO PR-2 DATA

These models are fit to the 13.4 and 35.6 GHz measured PR-2 profiles in the melting layer. The stationary assumption is used to determine the number distribution of drops of diameter  $D$  in the melting layer,

$$N_m(D) = N_w(D)V_w(D)/V_m(D) \quad (2)$$

so the only input needed to model the reflectivity profile in the melting layer is the drop size distribution at the base of the melting layer. The velocity of the melting particle  $V_m$  and the velocity of the rain drop  $V_w$  are given in Battaglia et al. (2003). The drop size distribution retrievals at the base of the melting layer are used as inputs to several of the melting layer models. An example of the melting layer model fits for both frequencies is shown in Figure 2.

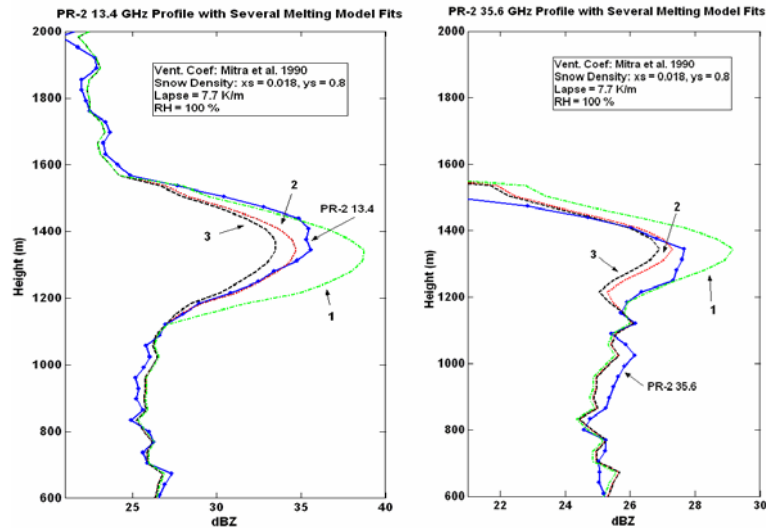


**Figure 2.** Fitting the melting layer models to the 13.4 (left) and 35.6 (right) PR-2 reflectivity profiles. Model 1 is {ice inclusions water matrix} | air, model 3 is air | {ice inclusions water matrix} and model 2 is the FS model with core (model 1) and shell (model 2).

It can be seen in figure 2 that the FS core shell model fits the PR-2 data well. Table 1 provides a summary of the statistics for the different dielectric models for approximately 100 profiles with basal reflectivities of 25 – 31 dBZ. The best fit, in terms of the 13.4 peak bias, using different snow densities and ventilation coefficients is shown for each dielectric model. The peak bias is the model reflectivity peak minus the PR-2 reflectivity peak. The width difference is the standard deviation of the model minus the standard deviation of the measurement. The fraction of the opacity is the fraction of the total atmospheric extinction at 10.7 GHz due to the melting layer. The mean wind speed is the average retrieved wind speed. It can be seen that models 1 and 2, which overestimate the scattering, also overestimate the total atmospheric absorption. The average wind speed outside the rain, as determined from the radiometer, is approximately 9-10 m/s.

The model that produced the best agreement with the PR-2 data is that which blends MG mixing formulas, such as the FS core shell model. This model was applied to the wind and rain retrievals. The retrieval using the FS core shell model is shown in Figures 3 – 6. Figure 3 shows the vertical profile of the 13.4 GHz reflectivity, showing a strong melting layer in the middle of the image. The retrieved wind speed without absorption from the melting layer is shown in Figure 4. Anomalously high wind speeds are observed where the melting layer is intense. Figure 5 shows the rain layer averaged rain rate retrieval from the radar for this storm. The rain rates are light, around 1 – 2 mm/hr, which means the 10.7 GHz absorption is mainly coming from the melting layer, as observed in Figure 1. Figure 6 shows the retrieved wind speed using the FS dielectric model. It is observed that this model is able to fit the PR-2 reflectivity profiles as well as produce reasonable radiometric wind speed retrievals. The resulting wind speed retrieval in stratiform rain decreased

by 30 to 40 % as compared to no melting layer absorption, and the rain rate retrieval increased by about 10 %.

Dielectric Formula	13.4 Peak Bias (dB)	35.6 Peak Bias (dB)	13.4 Width Dif. (dB)	Fraction of Opacity	Mean Wind Speed
(1) {Water   { air inclusions in ice matrix}}	5.2	3.1	1.4	0.72	0.03
(2) {ice inclusions   water matrix}   air}	3.8	2.5	1.0	0.66	0.63
(3) Fabry-Szyrmer Core-Shell	-0.3	0.23	0.37	0.45	9.9
(4) { air   {ice inclusions water matrix}}	-1.1	-0.43	-0.23	0.43	10.3
(5) {air inclusions in ice matrix}   water	-2.3	-0.54	-0.52	0.32	12.1

**Table 1.** Fit to PR-2 data for different dielectric models.

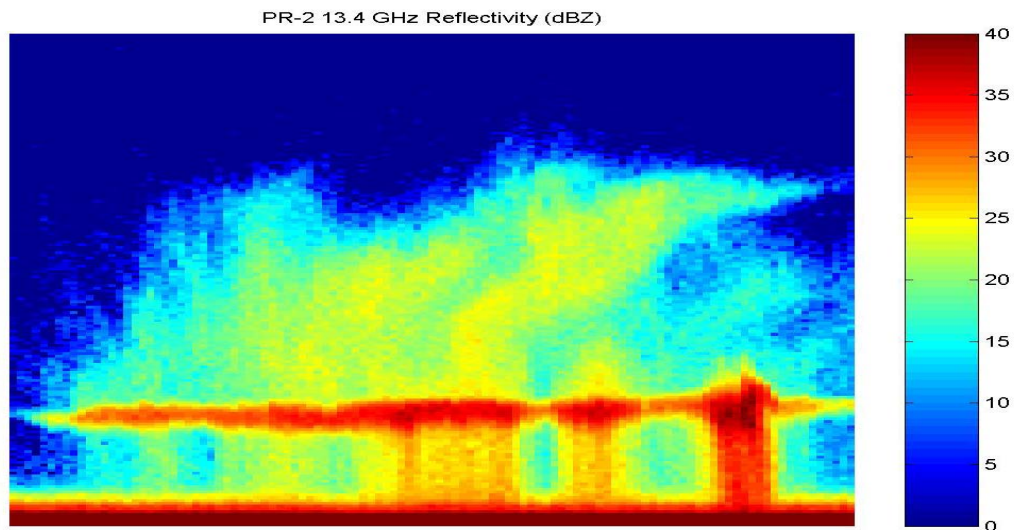


**Figure 3.** 13.4 GHz reflectivity for a stratiform rain case. The melting layer is approximately at 1500 m above the surface.

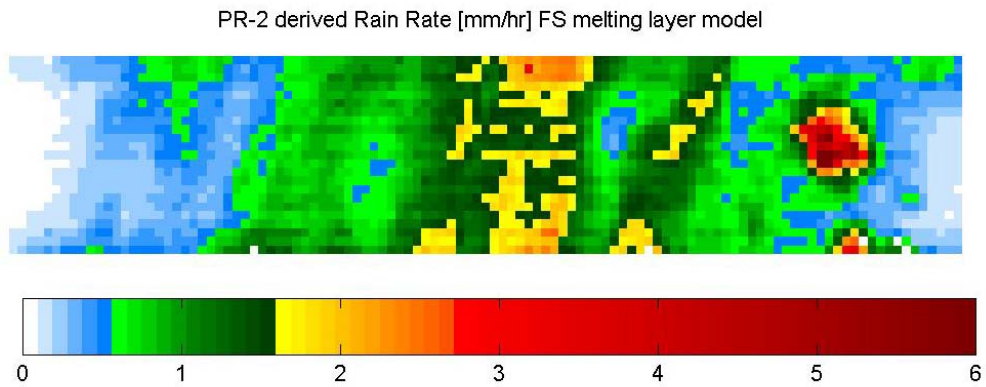


**Figure 4.** Rain rate retrieval using FS core shell model.

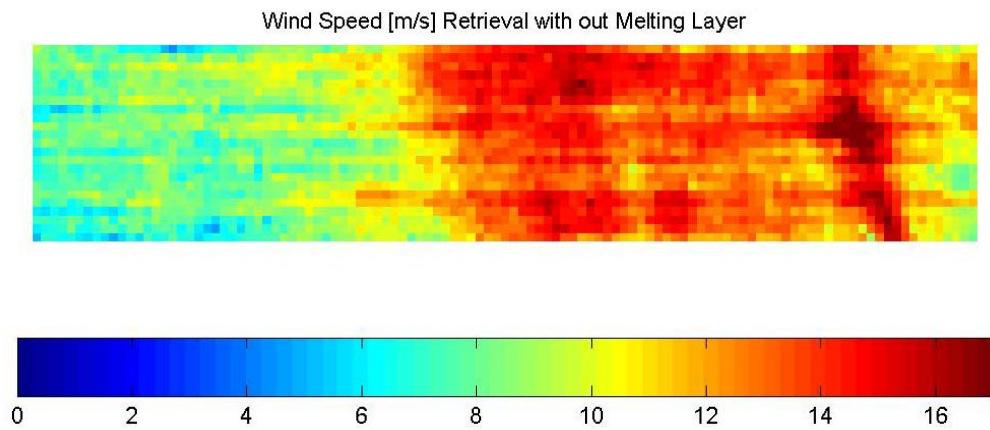


**Figure 5.** Wind speed retrieval without absorption from melting layer.

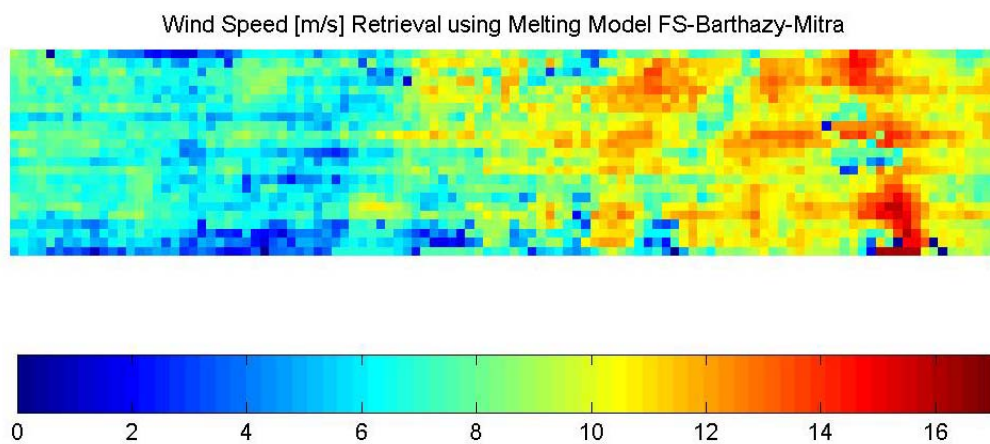


**Figure 6.** Wind speed retrieval using FS core shell model.

## 5. CONCLUSIONS

A retrieval algorithm is developed which uses dual-frequency radar backscatter measurements to profile the drop size distribution. The drop size distribution is used to determine the rain rate and liquid water content profile. The surface wind speed is estimated from the measured emissivity of the sea at 10.7 GHz, where the atmospheric clearing of the brightness temperature comes from the absorption and extinction coefficient profiles determined from the DSD. In stratiform rain, the retrieval is driven by the absorption in the melting layer. This requires an accurate model for the melting layer. Several models were fit to the PR-2 data, and the Fabry and Szyrmer core shell model was selected as the candidate model for the algorithm. Anomalous high wind speed retrievals with no melting layer were reduced by 30 to 40 % with the addition of the melting layer model and the radar retrieved rain rates were increased by 10 %.

## 6. REFERENCES

- Battaglia, A., C. Kummerow, D. Shin and C. Williams. 2003. Constraining Microwave Brightness Temperatures by Radar Brightband Observations. *J. Atmos. and Oceanic Tech*, **20**, pp 856-871.
- Bauer, P., A. Khain, A. Pokrovsky, R. Meneghini, C. Kummerow, F. Marzano and J. Baptista. 2000. Combined Cloud-Microwave Radiative Transfer Modeling of Stratiform Rain. *J. Atmos. Sci.*, **57**, pp 1082-1104.
- Bauer, P. J. Baptista and M Iulis. 1999. The Effect of the Melting Layer on the Microwave Emission of Clouds over the Ocean. *J. Atmos. Sci.*, **56**, pp 852-867.
- Bohren, C. and L. Battan. 1982. Radar Backscattering of Microwaves by Spongy Ice Spheres. *J. Atmos. Sci.*, **39**, pp 2623-2628.
- Fabry, F. and W. Szyrmer. 1999. Modeling of the Melting Layer. Part II: Electromagnetic. *J. Atmos. Sci.*, **56**, pp 3593-3600.
- Hitschfeld W. and J. Bordan. 1954. Errors Inherent in the Radar Measurement of Rainfall at Attenuating Wavelengths. *J. of Meteor.*, **11**, pp 58-67.
- Klassen, W. 1988. Radar Observations and Simulation of the Melting Layer of Precipitation. *J. Atmos. Sci.* **45**. 3741-3753. *J. Atmos. Sci.*, **56**, pp 852-867.
- Mitra, S. O. Vohl, M. Ahr and H. Pruppacher. 1990. A Wind Tunnel and Theoretical Study of the Melting Behavior of Atmospheric Ice Particles. IV: Experiment and Theory for Snow Flakes. *J. Atmos. Sci.*, **47**, pp 584-591.
- Olson, W., P. Bauer, N. Viltard, D. Johnson, W. Tao, R. Meneghini and L. Liao. 2001. A Melting-Layer Model for Passive/Active Microwave Remote Sensing Applications. Part I: Model Formulation and Comparison with Observations. *J. Appl. Meteor.*, **40**, pp 1145-1163.
- Pandey, P. and R. Kakar. 1982. An Empirical Microwave Emissivity Model for a Foam-Covered Sea. *IEEE J. Oceanic. Eng.*, **7**, pp 135-140.
- Szyrmer W. and I. Zawadzki. 1999. Modeling of the Melting Layer. Part I: Dynamics and Microphysics. *J. Atmos. Sci.*, **56**, pp 3573-3592.